RZ 3960 (#ZUR1607-024) 07/11/2016
Electrical Engineering 2 pages

Research Report

InGaAs-on-Si (Ge) 3D Monolithic Integration for CMOS and More-than-Moore Technologies

V. Deshpande[1], V. Djara[1], T. Morf[1], P. Hashemi[2], E. O'Connor[1], K. Balakrishnan[2], D. Caimi[1], M. Sousa[1], J. Fompeyrine[1] and L. Czornomaz[1]

[1] IBM Zurich Research Laboratory, Säumerstrasse 4, CH-8803 Rüschlikon, Switzerland

[2] IBM T.J.Watson Research Center,1101 Kitchawan Rd., Route 134 Yorktown Heights, NY, USA

This is the accepted version of the article published as: V. Deshpande, V. Djara, T. Morf, P. Hashemi, E. O'Connor, K. Balakrishnan, D. Caimi, M. Sousa, J. Fompeyrine and L. Czornomaz, "InGaAs-on-Si (Ge) 3D Monolithic Integration for CMOS and More-than-Moore Technologies," in Book of Extended Abstracts, 2016 Int'l Conf. on Solid State Devices and Materials (SSDM).

InGaAs-on-Si (Ge) 3D Monolithic Integration for CMOS and More-than-Moore Technologies

V. Deshpande[1], V. Djara[1], T. Morf[1], P. Hashemi[2], E. O'Connor[1], K. Balakrishnan[2], D. Caimi[1], M. Sousa[1], J. Fompeyrine[1] and L. Czornomaz[1]

[1] IBM Zurich Research Laboratory, Säumerstrasse 4, CH-8803 Rüschlikon, Switzerland
[2] IBM T.J.Watson Research Center,1101 Kitchawan Rd., Route 134 Yorktown Heights, NY, USA.

Abstract

3D Monolithic (3DM) integration can provide both density scaling benefits and the possibility to stack independently optimized layers at transistor level. However, top layer thermal budget poses a considerable challenge in such a technology. Due to its inherently low process temperature, InGaAs is well-suited to be used as the top layer channel material. Therefore, InGaAs has the potential to enable both low voltage-high performance advanced CMOS, as well as high-frequency device for RF/mixed-signal applications. In this regard, we show here our recent progress in InGaAs-on-SiGe 3D Monolithic technology, demonstrating state-of-the art device integration on both levels, DC and RF characterization top layer InGaAs nFETs and integrated inverters with sub-50 nm L_g down to V_{DD} = 0.25 V.

1. Introduction

3D Monolithic (3DM) integration is attracting much attention owing to density scaling benefits and the potential to stack independently optimized multifunctional layers at transistor level [1]. Typical Si MOSFET process has high thermal budget, requiring development of low temperature top layer Si/SiGe process for a 3DM scheme and thus presents challenges to obtain high-performance MOSFETs. On the other hand, the InGaAs MOSFET processing thermal budget is significantly lower, making it well-suited to be used as the top layer channel material. Moreover, InGaAs also has higher mobility which enables high performance at lower voltages [2] and is an excellent channel material for high-frequency devices enabling very high cut-off frequency. This aspect is of great interest as it can enable a truly multifunctional 3D monolithic integration scheme. On one hand, InGaAs nFETs on top of Si/SiGe FETs can allow higher performance hybrid CMOS [3] and on the other, high frequency InGaAs RF-FETs can benefit from closely integrated CMOS circuits [4]. As a step towards such a multi-functional 3D monolithic integration, here, we show DC and RF characteristics of InGaAs nFETs fabricated with RMG process on top of SiGe-OI finFETs. A cut-off frequency of 16.4 GHz for gate length (L_g) of 120 nm is obtained. We also show integrated inverters with sub-50 nm L_g down to V_{DD} = 0.25 V in the same stack. Robustness of the technology is demonstrated by the fact that impact on the bottom pFET performance is negligible, despite the top nFET RMG process featuring a self-aligned raised source drain epitaxy (with relatively high thermal budget).

2. Device Integration

The 3DM process flow is described in detail in ref. (3). Firstly, bottom layer SiGe-OI fin pFETs are fabricated with a process described in ref [5]. After the silicidation step of SiGe-OI finFET process, the inter-layer oxide is deposited and CMP planarization is carried out. The InGaAs layer is transferred on to this oxide with direct wafer bonding from InP donor wafers [6]. InGaAs nFET fabrication is then performed with the RMG process described in [7]. Finally, oxide encapsulation is deposited and contact holes are opened and metallization is completed. The schematic of the 3DM stack is shown in fig 1.

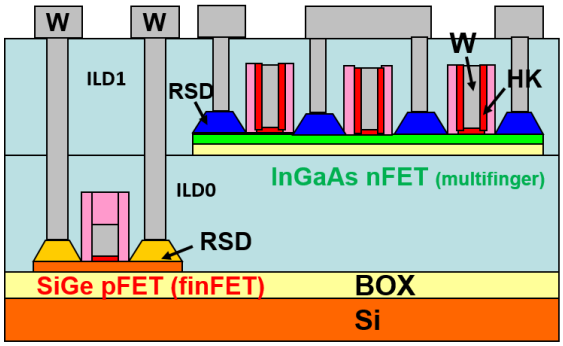

Fig. 1. Schematic the InGaAs-on-SiGe 3DM stack showing nFETs on top of SiGe finFETs.

3. Electrical Characterization

DC characteristics and circuits

Figure 2 shows the DC I_d - V_g characteristics of top layer InGaAs nFET with L_g = 70 nm, demonstrating competitive DC performance after the 3DM fabrication.

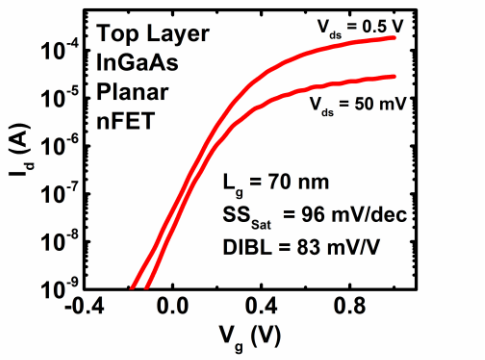

Fig. 2: I_d - V_g of InGaAs planar nFET on the top layer. The device features RMG, which yields very good electrostatics (SS_{sat} = 96 mV/dec, DIBL = 83 mV/V @ L_g = 70 nm).

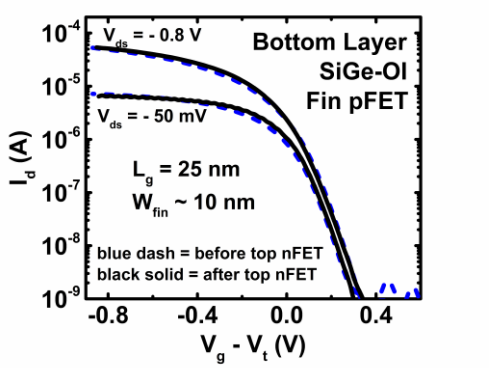

Fig. 3: I_d - V_g of SiGe-OI fin pFET before and after top nFET fabrication. Very similar I_{dsat} is obtained without degradation of electrostatics after top nFET fabrication. *This highlights the robustness of InGaAs-on-Si/SiGe 3DM technology*.

Figure 3 shows comparison of bottom SiGe-OI pFET I_d-V_g before and after top nFET fabrication. Nearly identical I_{dsat} is obtained post-nFET fabrication, indicating negligible impact on pFET silicide. The electrostatics of the device are also have very minimal change demonstrating low impact on the gate oxide and source/drain doping profile. This shows the robustness of the process and demonstrates the potential to achieve optimized performance on both, top-nFET and bottom-pFET layers.

Figure 4 shows the the voltage transfer characteristics (VTC) of scaled 3D inverters with nFET L_g = 80 nm (with pFET L_g ~ 30 nm) and L_g ~ 30 nm (for both nFET and pFET). Well-behaved transitions are obtained down to V_{DD} = 0.25 V, demonstrating that an optimized low-voltage CMOS can be achieved with InGaAs-on-SiGe 3DM technology.

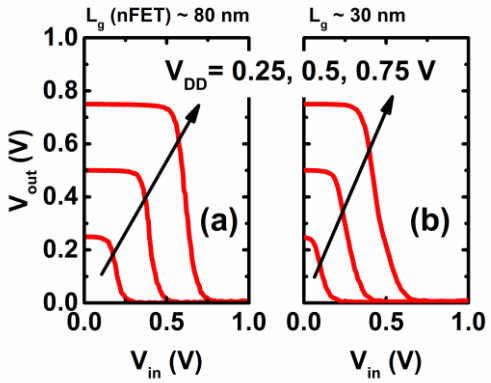

Fig. 4: Voltage transfer characteristics (VTC) of 3DM inverter. Well behaved characteristics are observed down to V_{DD} = 0.25 V owing to independent optimization of top InGaAs nFET and bottom SiGe-OI pFET. In (a) L_g ~ 80 nm in nFET and ~30 nm in pFET, while in (b) L_g ~ 30 nm in both nFET and pFET.

RF characteristics of top layer InGaAs nFETs

The top layer InGaAs nFETs used for RF characterization feature multi-finger gate structure [8] and have a gate-contact spacing of 100 nm. Multifinger gate layout allows lowering the gate-resistance. The measured current gain (after on-chip de-embedding) for a nFET with L_g = 120 nm and 10 gate fingers is shown in fig. 5. A cut-off frequency (F_t) of 16.4 GHz is obtained. Figure 6 shows cut-off frequency vs. gate length. As expected cut-off frequency is observed to increase with lower L_g. Further optimization of layout and device design would allow for higher F_t.

.

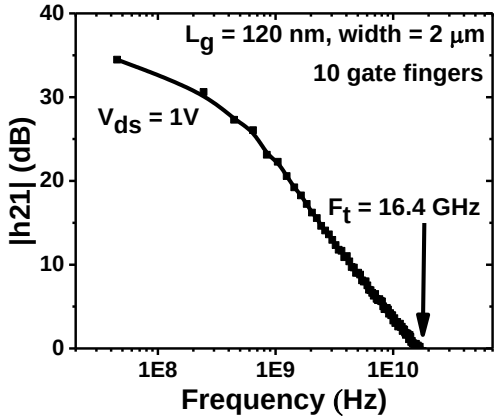

Fig. 5. Measured current gain (|h21|) vs. frequency for a InGaAs nFET (top layer) with L_g = 120 nm and 10 parallel gate fingers. Cut-off frequency (F_t) of 16.4 GHz is obtained for V_{ds} = 1V.

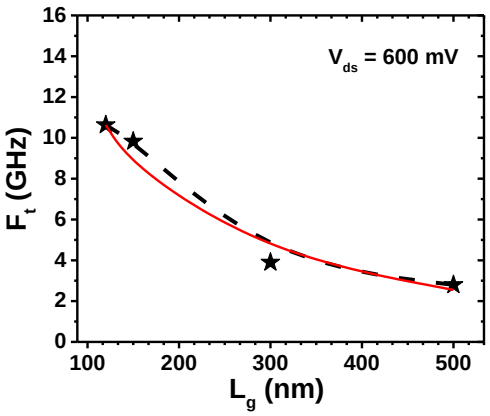

Fig. 6. Cut-off frequency vs. gate length (L_g) for top InGaAs nFETs for V_{ds} = 600 mV.

4. Conclusions

A robust InGaAs-on-Si(Ge) 3D Monolithic integration scheme is demonstrated that allows low voltage high-performance CMOS circuits as well RF-over-CMOS circuits. Owing to inherent benefits of low thermal budget and high mobility InGaAs as top layer enables optimized performance at both layers. Thus building blocks for a high performance, multi-functional 3D Monolithic technology is demonstrated.

Acknowledgements: Funding from the EU (ICT-2013-11 COMPOSE3, ICT-2013-11 IIIVMOS, H2020-ICT-2015-688784-INSIGHT and PEOPLE-2013-IEF FACIT).

References: [1]P. Batude, *et al.*, pp. 166-167, VLSI Tech. Symp. (2009). [2] M. Radosavljevic, *et al.*, IEDM (2011) [3]V. Deshpande, *et al.*, IEDM (2015). [4]T. Ge, *et al.*,pp. 94-97, Procedia Engineering (2016). [6]P. Hashemi, *et al.*, pp.1-2, VLSI Tech. Symp. (2014).[7]L. Czornomaz, *et al.*, pp. 23.4.1 - 23.4.4, IEDM (2012).[8]V. Djara, *et al.*, EDL, 37, 2, pp. 169-172(2016) [9]V. Deshpande, et. al., EuroULIS2016